

The Equivalence Theorem and infrared divergences

Tibor Torma*

June 14, 2018

hep-ph/9510217

Abstract

We look at the Equivalence Theorem as a statement about the absence of polynomial infrared divergences when $m_W \rightarrow 0$. We prove their absence in a truncated toy model and conjecture that, if they exist at all, they are due to couplings between light particles.

*e-mail: kakukk@phast.umass.edu

I Introduction

The Equivalence Theorem [1], from a practical point of view, is a tool to simplify calculations in spontaneously broken gauge theories. It states that, in the limit $\frac{\sqrt{s}}{m_W} \rightarrow \infty$, amplitudes with external longitudinal W_L 's and Z_L 's can be replaced by the corresponding (unphysical) Goldstone boson amplitudes. With this replacement one gains a simplification in Lorentz indices and calculations are simplified by the lack of gauge cancellations.

The early incomplete proofs of the Equivalence Theorem within the standard model [1] were improved using power counting arguments [2, 3]; see also [4]. One distinguishes two regimes, the light-Higgs regime with $\sqrt{s} \gg m_H, m_W, m_f$ and a heavy-Higgs regime with $m_H \sim \sqrt{s} \gg m_W, m_f$; in both cases excluding situations with exceptional momenta $((p_i - p_j)^2 \ll E^2)$ which could upset the power counting. The power counting proof of the Equivalence Theorem as given in [2] works to all orders; it also shows that in the heavy-Higgs regime all Feynman diagrams with lines in loops other than Goldstone scalar are subleading, allowing for a consistent truncation of Feynman amplitudes to pure Goldstone dynamics.

In this paper we discuss a possible flaw in the power counting proof which can occur if there are power-like infrared divergences. We argue that these do not occur in the minimal Higgs sector of the Standard Model, and use a toy model to argue that they are probably not present in its multi-Higgs extensions either.

C. Grosse-Knetter's argument [2] involves counting powers of m_H and $E = \sqrt{s}$ simultaneously. One starts with the well-known statement that $\langle phys | T F_1 \dots F_n | phys \rangle = 0$ for the R_ξ -gauge fixing terms $F_i = A_i^\mu - i g \xi \cdot \partial^\mu \Phi_i \rightarrow 0$, connecting matrix elements of the Goldstone bosons ϕ_i to vector bosons with (unphysical) polarization $\propto \frac{p^\mu}{m_V}$. Then one is to prove that the difference between the polarization vectors of these V 's and the longitudinal V_L vector bosons, $v^\mu = \epsilon^\mu - \frac{p^\mu}{m_V} \equiv \frac{m_V}{E_V + p_V} \cdot (1 | \mathbf{0})^\mu$ gives only subleading contributions in the appropriate limit. A generic Feynman amplitude is, explicitly displaying the E and m_H factors, a sum of terms, each in the form

$$\mathcal{M} = c \cdot E^{\frac{E_f}{2} - E_v} \cdot m_H^{2V_\Phi} \cdot I_F, \quad (1)$$

where the constant c may depend on the m_V 's, V_Φ is the added number of Φ^3 and Φ^4 Higgs self-interactions, E_f is the number of external fermions and

E_v is the number of v^μ 's; the remaining part of the Feynman amplitude is in the general form

$$I_F = \int d^{4L}k \cdot \frac{p \cdots p}{(q_1^2 - m_1^2) \cdots (q_I^2 - m_I^2)}, \quad (2)$$

where we collectively denoted by p and q the occurring linear combinations of external and loop momenta; m denotes both the heavy and the light masses.

Eqn. 2 is a general formula for all processes and should include all internal lines present in the theory. As explained below, an assumption on its behavior in general at large scales can be used to prove the Equivalence Theorem. For this purpose, the relevant graphs are those which include at least one external longitudinal vector boson.

If we now suppose that I_F is determined by the scale E and m_H , we have

$$I_F = m_H^D \cdot f_0\left(\frac{E}{m_H}\right) + m_H^{D-1} \cdot m_W \cdot f_1\left(\frac{E}{m_H}\right) + \dots \quad (3)$$

with dimensionless f_j (possibly containing logarithms of m_W and of the renormalization scale but no powers of $\frac{1}{m_W}$) easy combinatorics shows that the total power of E and m_H , counted simultaneously, in \mathcal{M} is at most

$$N = (2L + 2) - (V_d + 2V_0 + V_f + E_v) \quad (4)$$

where L is the number of loops, V_d and V_f are the numbers of derivative and fermion couplings respectively; $V_0 = V - V_\Phi - V_d - V_f$. This formula shows that the leading graphs are, at each loop level, those with $E_v = 0$ (i.e. proves the Equivalence Theorem) and also shows that no vector or fermion lines are involved in loops in leading graphs. The former statement can also be proven true for the light-Higgs regime using a similar argument.

A possible flaw in this argument can occur if negative powers of the light mass m_V enter the expansion (3). That expression can be viewed as an infrared statement: up to possible logarithmic factors involving the renormalization scale, we can fix the unit of dimension at E (or at $m_h \propto E$), to get a theory with $m_V \rightarrow 0$, wherein m_V acts as an infrared regulator. Then, the statement in (3) has been transformed into the statement that *the leading part of a graph, f_0 , does not pick up polynomially divergent factors when $m_V \rightarrow 0$* . In many calculations of IR divergent quantities that use a small regulator mass (for examples, see [5, 6] among many others) one finds that

the divergences are only logarithmic in the regulator mass and this is the basis for the expansion in (3). Any infrared divergences of the polynomial type in $\frac{1}{m_V}$ would introduce additional factors of $\frac{m_H}{m_V}$ and/or $\frac{E}{m_V}$ and such terms would invalidate the above proof which is based on their absence. To see if any such factor actually upsets the Equivalence Theorem one needs to analyse by how many powers of m_V the graph in question is suppressed in (3). For example, $V_L V_L \rightarrow V_L V_L$ at one loop has $\left(\frac{m_W}{E \text{ or } m_W}\right)^4$, i.e. $N = -4$ as leading behavior. Any additional factor of $\frac{1}{m_V}$ in, say, the box diagram of Fig. 1, which itself is one of the leading graphs, would introduce a factor that breaks the Equivalence Theorem.

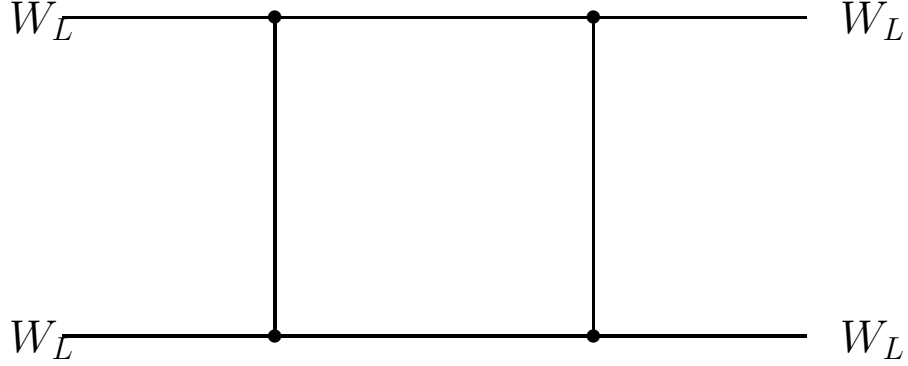


Figure 1: One of the leading graphs that might pick up IR divergences at 1-loop level.

A related problem could occur in a theory with several Higgses when some of them are heavy and at least one is light. Powers of $\frac{1}{m_h}$ for the light Higgs could upset the power counting.

What the argument in [2] does is, in this light, that it shifts the question of 'breaking' the Equivalence Theorem to the question of the presence of severe (i.e. polynomial) IR divergences.

This point of view is in accordance with the view that the Equivalence Theorem expresses the fact that Goldstone d.o.f's are turned into longitudinal

vector bosons by a spontaneously broken gauge transformation. With fixed E and $m_V \rightarrow 0$ we approach the point of phase transition where the t'Hooft gauge condition $\partial_\mu V^\mu = m_W \cdot \phi$ turns from a way to express ϕ with V_L into the physicality condition on V_L . The $m \rightarrow 0$ limit of a vector boson is a notoriously tricky problem. Whether the transition is smooth enough not to break the relations between amplitudes or not, will show up in the presence or lack of 'bad' IR divergences.

In this paper we argue that such divergences do not occur in the pure Higgs sector, at least, for non-exceptional momenta. We try to relate the IR divergence found in scalar box graphs (see Eqn. (5) below to the Equivalence Theorem and find no such divergence when the external particles are massive. In the conclusion we point out that a similar treatment is necessary for massless external particles which requires an analysis more similar to the case of the IR divergences in QCD. Experience with graphs involving massless particles of different spins shows that the infrared divergences of a diagram are generally determined by the denominators in the integrals of Eqn. (2) and the presence of spin affects only the numerators in that expression. The result is that the general structure of the IR divergences is independent of the spin (see e.g. [5, 6]) and the reason is the following. IR divergences come from specific points in the loop integration region where 4-momenta k^μ of some massless propagators vanish. One can then expand the numerators around those points in k . We see that in terms of higher order in k , IR divergences cancel and the remaining divergent part involves only a constant, i.e. a structure that is similar to the spin-0 case. This argument tells us that the absence of IR divergences in the scalar sector essentially proves the absence of divergences in the full model. One might hope that for some theories one could get special behavior from the numerators for special reasons, such as gauge invariance, that might remove an IR divergence that would otherwise be present. However, the scalar theory then would only be worse, so that by exploring the scalar theory one should be able to find the strongest divergences.

The situation here is analogous to QED in that interactions of massive particles through massless photons (the latter now correspond to the W and Z) introduce only logarithmic IR divergences. To complete the proof of the Equivalence Theorem to all orders one should also prove that in a situation more reminiscent of QCD, where massless gluons (now corresponding to W and Z) introduce IR divergences that are much harder to handle, polynomial

IR divergences are also absent – a question we do not address here.

The form of IR divergences of Feynman graphs has been calculated in QED many times (see, e.g. Zwanziger [5]), and is usually found to be logarithmic in the various IR regulators to any finite order. It has been calculated [6] for gravitons with similar results. However, it is well-known that in the nonrelativistic limit scalar box graphs, such as that in Fig. 2. pick up $O\left(\frac{1}{m^2}\right)$ terms for forward scattering [7]:

$$i\mathcal{M} \sim \frac{1}{m^2 M(p + \frac{i}{2}m)} \quad (5)$$

clearly showing the type of behavior expected to break the Equivalence Theorem. It is worth to note, however, that these calculations use either a small off-shellness parameter [5] $\varepsilon_i = p_e^2 - m_e^2$ or an explicit cutoff [6] $|p_\gamma^0| < \lambda$ as an IR regulator, so they are not directly relevant to our case where a small regulator mass m should be used.

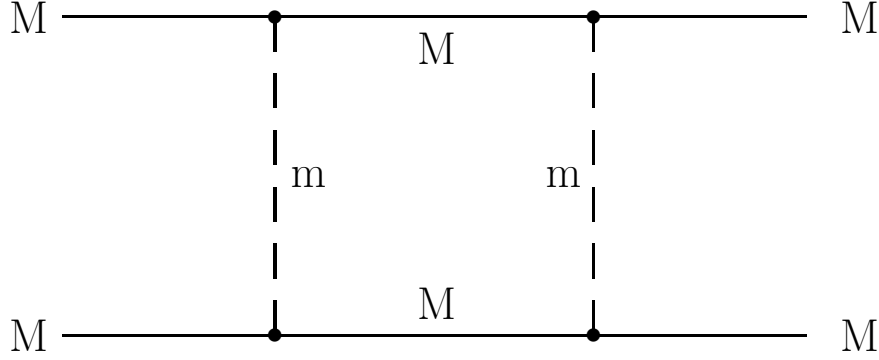


Figure 2: One-loop graphs with powerlike $\frac{1}{m}$ behavior.

It is an interesting coincidence that the structure in Fig. 2. is not present in the Standard Model. The only heavy mass there is $M \rightarrow m_H$ and there are no HHW or HHZ couplings (the absence of the latter is a consequence of separate C and P -conservation in the purely bosonic part of the SM, where

$J^{PC}(Z) = 1^{--}$). All other box graphs are less IR divergent because less internal lines can be put on shell in the same time.

The obvious way to look for a similar divergence is in the two-doublet Higgs model which possesses one heavy Higgs $M \rightarrow m_H$ and at least one light 0^{++} Higgs $m \rightarrow m_h \leq m_Z$. Even though such an IR divergence is not a genuine $\frac{1}{m_W}$, because of the necessary lightness of m_h , it affects the amplitudes in the same way.

In Sect. II we use Weinberg's method to analyse [6] the 'truncated MSSM model' to all orders, dropping all particles from there except the heavy and the light 0^{++} Higgses, using $m \rightarrow m_h$ as an infrared regulator. This model conserves the number of heavy H 's, which so act as 'charged' particles while the light h 's act as uncharged scalar photons. The lack of the coupling between light particles allows to extract the IR divergences in complete analogy to the QED case and we find only logarithmic divergences. The S -matrix elements pick up factors

$$S_{\beta\alpha} = S_{\beta\alpha}^{(0)} \cdot \exp \left\{ \frac{g^2}{4(2\pi)^2} \cdot (\mathcal{G} + i\mathcal{F}) \cdot \log \frac{\Lambda}{m} \right\} \quad (6)$$

where $2\pi g = Gm_Z$ is an MSSM coupling constant, $m \ll \Lambda \ll E$ is an energy when we separate soft particles from hard ones. \mathcal{F} has contributions from pairs of incoming and from pairs of outgoing H 's; \mathcal{G} has contributions from all pairs. As we will see in Sect. II, \mathcal{G} is canceled on the cross section level by real soft h 's; the \mathcal{F} does not contribute to the cross section but it shifts the Coulomb phase by an $\sim \log \frac{\Lambda}{m}$ term, thus explaining why there is no Coulomb phase contribution from a pair formed of one incoming and one outgoing H . In Sect. III we calculate explicitly the IR divergent contributions in $HH \rightarrow HH$ to one-loop level and find complete agreement with the above conclusions. It is of some interest how these IR divergent terms are separated using our small-mass regularization: one needs a careful and long procedure which is illustrated by describing the details for one particular diagram. The mechanism of the cancellation of IR divergences, all logarithmic in m , between loop integrals and soft 'photons' attached to heavy external legs closely follows the corresponding mechanism in $ee \rightarrow ee$ in QED, so it is straightforward to generalize the result of Sect. II for any other process in this toy model, for example, for $hH \rightarrow hH$ or $hh \rightarrow hh$, analogous to $e\gamma \rightarrow e\gamma$ or $\gamma\gamma \rightarrow \gamma\gamma$.

The total absence of powerlike divergences shows that the $\frac{1}{m^2}$ divergence of the nonrelativistic forward amplitude is due to exceptional momenta. This statement is in compliance with that the coefficient of our $\log \frac{\Lambda}{m}$ divergence itself diverges when two particles are collinear (see Eqn. (12), $\beta_{ij} \rightarrow 0$).

In Sec. II we show that in a simplified model with two scalars only no polynomial IR divergences occur. As a consistency check we show that the IR structure found is identical with the one necessary in order that soft Bremsstrahlung exactly cancels the IR divergences in loops. We then illustrate this general argument in Sect. III with a calculation of the relevant 1-loop amplitudes. In the conclusion we point out that the presence of coupled light particles (i.e. gauge boson self-coupling) introduces additional difficulties which require a separate investigation.

II The 'truncated MSSM' model

We use the H and h part of the MSSM as a toy model to illustrate why IR divergences are at most powers of logarithms in the small masses. This model has only one coupling (see Fig. 3) with a dimensionless $G \sim g_{weak}$; the m_Z factor in the coupling should not be considered as suppressing the IR divergence: *any* deviation in the expansion of I_F from Eqn. (3) upsets the power counting. In this model, with $M \rightarrow m_H$ and E kept constant and $m \rightarrow m_h$ sent to zero, we calculate the IR divergences, closely following the argument in Weinberg [6].

All the IR divergences in an *amplitude* stem from a set of soft h exchanges between external legs of Feynman graphs. Their factorization [6] is due to the fact that these corrections are attached to all graphs in the same way. We have, for each attached soft exchange (see Fig. 4.)

$$S_{\beta\alpha} = S_{\beta\alpha}^{(0)} \cdot \left\{ 1 + \int d^4q \cdot A(q) \right\} \quad (7)$$

and

$$A(q) = \frac{i}{(2\pi)^4} \cdot \int \frac{d^4q}{q^2 - m^2 + i\varepsilon} \cdot \frac{i(i \cdot 2\pi g)}{(p_1 + \eta_1 q)^2 - M^2 + i\varepsilon} \cdot \frac{i(i \cdot 2\pi g)}{(p_2 - \eta_2 q)^2 - M^2 + i\varepsilon} \quad (8)$$

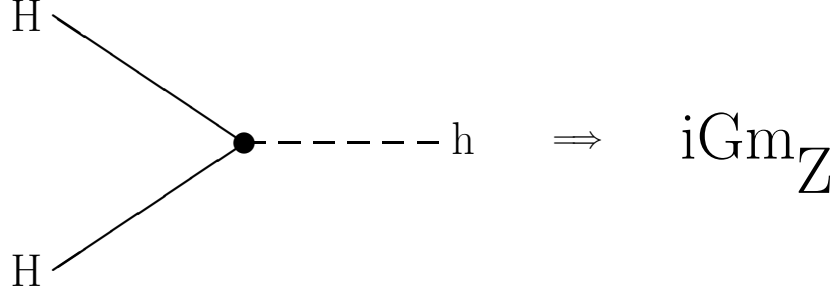


Figure 3: The only remaining vertex in the truncated MSSM.

and $\eta_j = +1$ (or -1) when the H is outgoing (incoming). Attaching all possible soft exchanges leads to a factorized amplitude [6]

$$S_{\beta\alpha} = S_{\beta\alpha}^{(0)} \cdot \exp \int d^4q \cdot A(q) . \quad (9)$$

The integration is over a $[-\Lambda, +\Lambda]$ range in q^0 with IR cut $\ll \Lambda \ll E$; the resulting Λ dependence is compensated by a Λ -dependence in the hard h part $S_{\beta\alpha}^{(0)}$. In addition, by the usual $|q^0| > 2$ cutoff we get, after some elementary integrations, with $m \equiv 0$:

$$A_\lambda = \frac{g^2}{8} \cdot \sum_{j \neq l} \frac{\eta_j \eta_l}{(p_j \cdot p_l)} \cdot \frac{1}{\beta_{jl}} \log \frac{1 + \beta_{jl}}{1 - \beta_{jl}} \quad (10)$$

where β_{jl} is the relative velocity of two H 's

$$\beta_{jl} = \sqrt{1 - \frac{M^4}{(p_j \cdot p_l)^2}} . \quad (11)$$

What we need is to use $m > 0$ instead of $\lambda > 0$; to calculate it we need a careful analysis of how complex singularities move around on the q^0

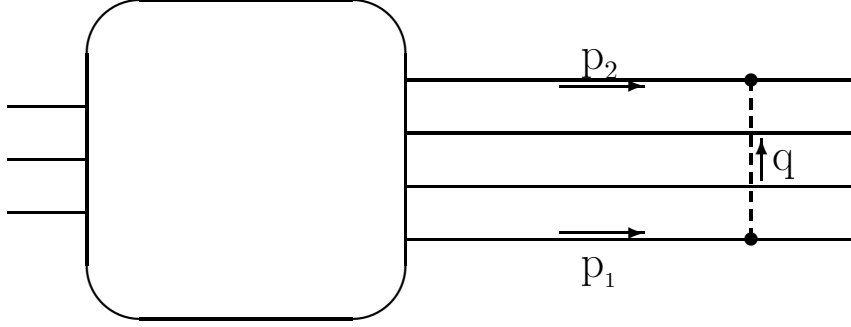


Figure 4: Attaching a soft exchange to external lines.

plane. Closing the contour around them and integrating over angular variables leaves us with one-dimensional integrals. Separating their IR divergent (i.e. when $m \rightarrow 0$) parts is a tedious calculation; we only quote the result in the form of Eqn. (6) with

$$\mathcal{G} = -2\pi^2 \sum_{j \neq l} \frac{\eta_j \eta_l}{(p_j \cdot p_l) \beta_{jl}} \cdot \log \frac{1 + \beta_{jl}}{1 - \beta_{jl}}$$

and

$$\mathcal{F} = \sum_{j \neq l \text{ with } \eta_j = \eta_l} \frac{(4\pi)^3}{(p_i \cdot p_j)^2 - M^4} . \quad (12)$$

In a physical process, the $\exp \left\{ i \cdot \frac{q^2}{4} \cdot \mathcal{F} \cdot \log \frac{\Lambda}{m} \right\}$ factor contributes to the Coulomb phase as we said in the introduction; the \mathcal{G} part goes into the cross section and gets compensated by real soft h 's.

One may always add any number of undetectably soft h 's to the initial and/or final states as long as their total energy is less than the energy resolution of the measuring device. Although this has not much practical sense for $m_h \sim 10$'s of GeV 's, we still see that a Bloch-Nordsieck-type cancellation occurs. Attaching N soft h 's to the external legs, the amplitude picks up an

IR divergent factor

$$S_{\beta\alpha}(\mathbf{q}_1, \dots, \mathbf{q}_N) = S_{\beta\alpha} \cdot \frac{1}{N!} \cdot \prod_{n=1}^N \sum_j \frac{i(i \cdot 2\pi g)}{(p_j - \eta_j \cdot q)^2 - M^4} . \quad (13)$$

These states should be added on the probability level as they represent orthogonal states. Using the factorization property as in [6] again, we get for the transition rate

$$\begin{aligned} \Gamma_{\beta\alpha}(\mathbf{q}_1, \dots, \mathbf{q}_N) &= |S_{\beta\alpha}|^2 \cdot \frac{1}{N!} \cdot \prod_{n=1}^N \frac{g^2}{16\pi E_{q_n}} \cdot \\ &\cdot \sum_{jl} \frac{\eta_j \eta_l}{[(p_j \cdot q_n) + \eta_j \frac{m^2 + i\varepsilon}{2}] [(p_l \cdot q_n) + \eta_l \frac{m^2 - i\varepsilon}{2}]} . \end{aligned} \quad (14)$$

Integrating this over the h 's' phase space with the restriction

$$\chi \left(\sum_{n=1}^N E_n \leq \Lambda \right) \equiv \frac{1}{\pi} \cdot \int_{-\infty}^{+\infty} \frac{d\sigma}{\sigma} \cdot \sin \sigma \cdot e^{i \frac{\sigma}{\Lambda} \cdot \sum_{n=1}^N E_n} \quad (15)$$

we have, with the total energy carried away by the h ' less than Λ :

$$\begin{aligned} \Gamma_{\beta\alpha}(\leq \Lambda) &= |S_{\beta\alpha}|^2 \cdot \frac{1}{\pi} \cdot \int_{-\infty}^{+\infty} \frac{d\sigma}{\sigma} \cdot \sin \sigma \cdot \\ &\cdot \exp \left\{ \frac{g^2}{16} \cdot \int_0^\infty \frac{dq \cdot q^2}{E_q} \cdot e^{i \frac{\sigma}{\Lambda} \cdot E_q} \cdot \right. \\ &\cdot \left. \sum_{jl} \oint_{4\pi} \frac{\eta_j \eta_l \cdot d^2 \underline{n}}{[(p_j \cdot q) + \eta_j \frac{m^2 + i\varepsilon}{2}] \cdot [(p_l \cdot q) + \eta_l \frac{m^2 - i\varepsilon}{2}]} \right\} . \end{aligned} \quad (16)$$

The separation of IR divergences requires a hard mathematical procedure that we do not present here; in essence, we write the integral

$$\begin{aligned} \int_0^\infty \frac{dq \cdot q^2}{E_q} \cdot e^{i \frac{\sigma}{\Lambda} E_q} &\implies \\ \implies \int_\Lambda^\infty \frac{dq \cdot q^2}{E_q} \cdot e^{i \frac{\sigma}{\Lambda} E_q} &+ \int_0^\Lambda \frac{dq \cdot q^2}{E_q} \cdot (e^{i \frac{\sigma}{\Lambda} E_q} - 1) + \int_0^\Lambda \frac{dq \cdot q^2}{E_q} \end{aligned} \quad (17)$$

and prove that the first two terms do not contribute to the IR divergence. Our result is

$$\Gamma_{\beta\alpha} = |S_{\beta\alpha}|^2 \cdot \exp \left\{ -\frac{g^2}{4(2\pi)^2} \cdot \mathcal{G} \cdot \log \frac{\Lambda}{m} \right\} \quad (18)$$

with the same \mathcal{G} as in Eqn. (12), proving the cancellation of all IR divergences in the transition probabilities.

Expanding any of our results in the coupling constant G shows that, to all orders, the worst divergence is only a power of $\log \frac{\Lambda}{m}$. We note that although summing up all orders we certainly get a powerlike behavior,

$$S_{\beta\alpha} = S_{\beta\alpha}^{(0)} \cdot \left(\frac{\Lambda}{m} \right)^{-\frac{g^2}{2(2\pi)^2} \cdot \mathcal{G}}, \quad (19)$$

we do not think this points to the breaking of the Equivalence Theorem; we are, after all, summing for a very particular set of diagrams.

III A one-loop example

In order to illustrate the results of Sect. II, and also to see how the IR divergences of particular diagrams add up, we work out the infrared divergences of $HH \rightarrow HH$ at one loop level and find complete agreement with Eqns. (6,12). Fortunately, all graphs with IR divergences are UV finite, so we may ignore renormalization. It turns out that each individual divergent graph has a $\log \frac{\Lambda}{m}$ divergence and no cancellations occur.

The IR divergent graphs are shown on Figs. 5,6. In addition to these, one must include tree graphs and add all h mass insertions to them; these graphs turn out to be IR finite though. The calculation of each individual IR divergent part is too complicated to explain here; we briefly describe one of them (the one corresponding to Fig. 5a in the Appendix). We simply quote the result in terms of I_{graph} :

$$i\mathcal{M}_{graph} = -\pi^2 \cdot g^4 \cdot \log \frac{\Lambda}{m} \cdot I_{graph} \quad (20)$$

and

$$I_{(4a)} = \frac{1}{E^2 \beta t} \cdot \left(\log \frac{1+\beta}{1-\beta} - i\pi \right) + (t \leftrightarrow u) \quad (21.1)$$

$$I_{(4b)} = -\frac{4}{t} \cdot \phi(u) + (t \leftrightarrow u) \quad (21.2)$$

$$I_{(4c)} = -\frac{4}{s} \cdot \phi(t) + (t \leftrightarrow u) \quad (21.3)$$

$$I_{(5a)} = \frac{1}{E^2 \beta s} \cdot \left(\log \frac{1+\beta}{1-\beta} - i\pi \right) \quad (21.4)$$

$$I_{(5b)} = -\frac{2}{t} \cdot \phi(t) + (t \leftrightarrow u) \quad (21.5)$$

with $E = \frac{1}{2}\sqrt{s}$; β is the relative velocity $\beta = \sqrt{1 - \frac{4M^2}{s}}$ and

$$\phi(x) \equiv \frac{4}{\sqrt{x(x-4M^2)}} \log \frac{\sqrt{4M^2-x} + \sqrt{-x}}{\sqrt{4M^2-x} - \sqrt{-x}}. \quad (22)$$

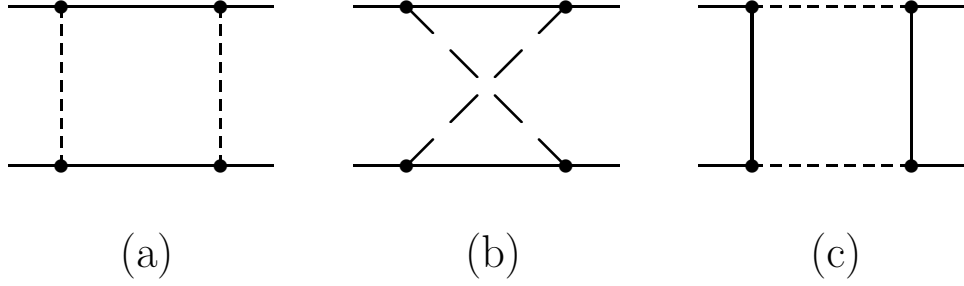


Figure 5: Infrared divergent box graphs in the truncated MSSM.

The sum of all these terms gives (with spacial momentum $p = \beta \cdot E$)

$$I_{total} = \left(\frac{1}{t} + \frac{1}{u} + \frac{1}{s} \right) \cdot \left\{ \frac{1}{Ep} \cdot \left(\log \frac{E+p}{E-p} - i\pi \right) - \phi(t) - \phi(u) \right\}. \quad (23)$$

This formula eventually coincides with what one gets from Eqns. (6,12). The tree level amplitude is

$$i\mathcal{M}_{tree} = (2\pi g)^2 \cdot \left(\frac{1}{t} + \frac{1}{u} + \frac{1}{s} \right) \quad (24)$$

and explicit use of Eqn. (12) allows us to arrive at the same Eqn. (23).

As an alternative way of calculation, we computed $I_{(4a)}$ by a dispersive calculation. In this calculation we used the usual Landau rules to show

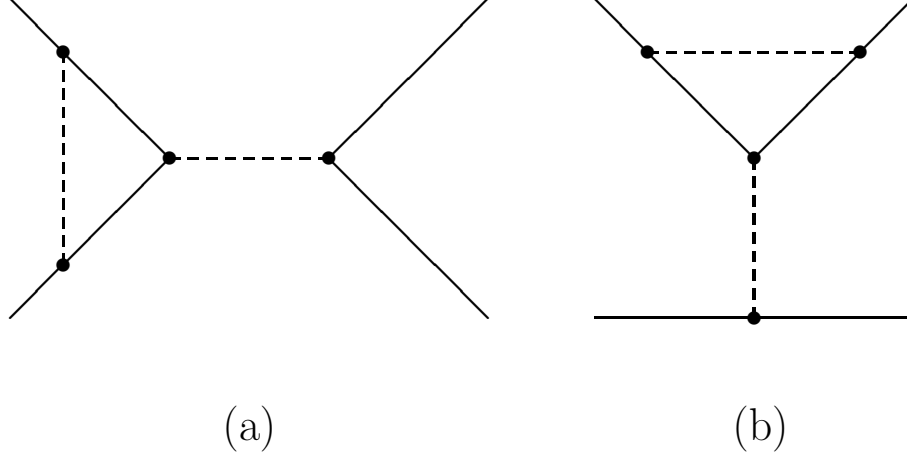


Figure 6: More infrared divergent one-loop graphs.

that this graph has no other singularities at fixed $t < 0$ in the complex s plane but a two- H cut from $4M^2$ to $+\infty$, corresponding to the cut graph on Fig. 7. The singularity for $4M^2 \leq s \leq 4M^2 - t$ is there in spite of the fact that the physical region for this process (we have fixed $t < 0$!) starts at $s \geq 4M^2 - t > 4M^2$. The discontinuity across this cut is calculated from the Cutkosky rules [8]

$$Im \{i\mathcal{M}_{(1a)}\} = g^4 \cdot \int d^4k \cdot \frac{(-i\pi)\delta^+[k^2 - M^2] \cdot (-i\pi)\delta^+[(p-k)^2 - M^2]}{[(k-p_1)^2 - m^2] \cdot [(k-p_2)^2 - m^2]}. \quad (25)$$

A straightforward calculation leads to

$$Im \{i\mathcal{M}_{(1a)}\} = -\pi^2 \cdot g^4 \cdot \frac{2\pi}{4Ep^3(1 - \cos \Theta)} \cdot \log \frac{E}{m} + O(1). \quad (26)$$

The real part of the amplitude is determined from the dispersion relation

$$i\mathcal{M}_{(box)} = \frac{1}{\pi} \cdot \int_{4M^2}^{\infty} \frac{ds'}{s' - s - i\varepsilon} \cdot Im \{i\mathcal{M}_{(1a)}(s', t)\}. \quad (27)$$

We note that no subtraction is needed and that we must include the contribution from unphysical $s' < 4M^2 - t$ where p is imaginary. Substituting Eqn. (26) into Eqn. (27) some elementary complex integrations lead to Eqn. (21.1).

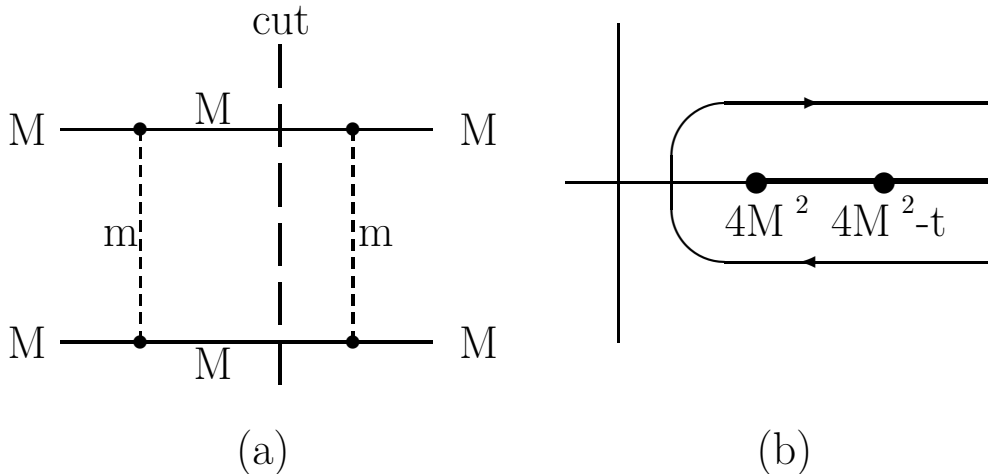


Figure 7: Singularities of the graph (5a) in the complex s plane for fixed $t < 0$.

This calculation, especially the coincidence of Eqns. (6,12) and (23) shows, through a particular example, the correctness of what we did in Sect. II.

IV Conclusion

We have shown, both by general argument and explicit example, that in diagrams involving scalar loops no powerlike infrared singularities occur. The introduction of spin does not alter this conclusion, and we use this result to show that the power coupling proof of the Equivalence Theorem put forward in [2] *does not suffer from IR divergences*. However, our reasoning allows us to arrive at this conclusion only in the massive sector, because the above analysis can break down when massless propagators are included into loop integrations (for our purposes, gauge bosons and/or light Higgses of the MSSM model are considered 'massless'.)

On the basis of these results we put forward the conjecture that, at least when the light particles are not coupled to each other — no worse IR divergences occur than $O\left(g^n \cdot \log^n \frac{\Lambda}{m}\right)$; we actually prove this in Sect. II. A general proof seems straightforward. The generalization for coupled light par-

ticles (which is certainly the case in the SM) needs a separate investigation. This case is in a sense similar to the analysis of IR divergences in QCD. One particular graph that could cause trouble is the same as the one one Fig. 1, with light particles on the internal lines. Yang-Mills theories certainly have bad IR behavior which ultimately leads to confinement; the corresponding investigation might involve an adaptation the methods used there.

Appendix: The calculation of $I_{(4a)}$

In this Appendix, as an illustration to the main ideas in all these similar calculations, we briefly describe the calculation of the IR divergent part in the box graph of Fig. 6a. The usual Feynman parameter integral is

$$i\mathcal{M}_{(1a)} = -\pi^2 \cdot g^4 \cdot \iiint_0^{x+y+z<1} \frac{dxdydz}{\{J_m(x, y, z) - i\varepsilon\}^2} \quad (28)$$

with

$$\begin{aligned} J_m(x, y, z) &= m^2 \cdot (x + y) + M^2 \cdot (1 - x - y)^2 \\ &\quad - s \cdot z(1 - x - y) - t \cdot xy . \end{aligned} \quad (29)$$

A change of integration variables to $u = 1 - x - y$, $v = \frac{4xy}{(x+y)^2}$ and $w = 1 - \frac{2z}{1-x-y}$ allows us to have a form

$$J_m = m^2 \cdot (1 - u) + M^2 \cdot u^2 + \left(\frac{1 - u}{2}\right)^2 \cdot v - s \cdot u^2 \cdot \frac{1 - w^2}{4} \quad (30)$$

in which all the u and v singularities are on the upper complex half plane. We change both contours to ones in the lower half plane as shown on Fig. 8.

We then treat each of the resulting six integrals in turn. As an example, we take the parts with $v \equiv -i\bar{v} : (-i \rightarrow 0)$ and $w \equiv 1 - i\bar{w} : (1 - i \rightarrow 1)$:

$$i\mathcal{M} \Rightarrow -\frac{\pi^2}{2} \cdot g^4 \cdot \int_0^1 du \cdot u \cdot (1 - u) \cdot \int_0^1 \frac{d\bar{v}}{\sqrt{1 - i\bar{v}}} \cdot \int_0^1 \frac{d\bar{w}}{(J_m - i\varepsilon)^2} \quad (31)$$

with

$$\begin{aligned} J_m &= \left[m^2 \cdot (1 - u) + u^2 \cdot (M^2 - E^2 \cdot \bar{w}^2) \right] \\ &\quad - i \cdot \left[\left(\frac{1 - u}{2}\right)^2 \cdot \bar{v} + 2E^2 \cdot u^2 \cdot \bar{w} \right] \end{aligned} \quad (32)$$

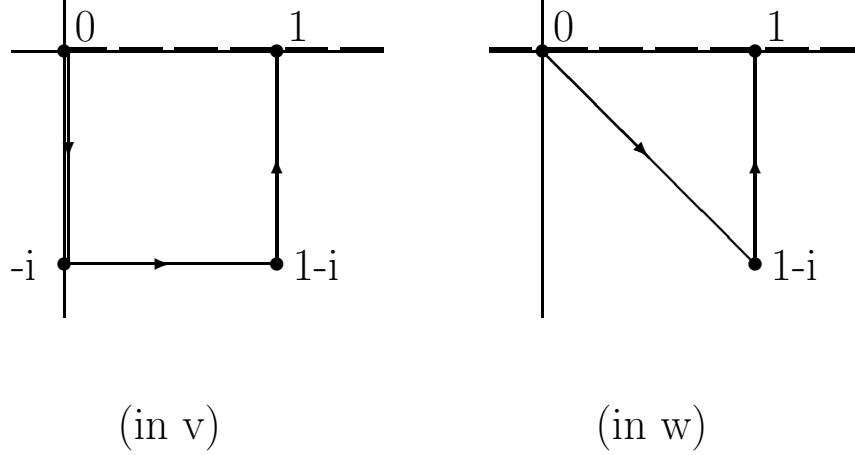


Figure 8: Avoiding singularities in the Feynman parameters v and w on the complex plane. The dashed line represents the possible positions of singularities.

(we set the unit of mass to $\sqrt{-t} \Rightarrow 1$).

Next we break up the u integration as $\int_0^{1/2} du + \int_{1/2}^1 du$ and (using Lebesgue's theorem) show that the second is IR regular. In the first term, a second order Taylor formula for $\frac{1}{\sqrt{1-i\bar{v}}}$ allows to drop the remainder term and we are left with (dropping all IR finite terms)

$$\begin{aligned}
 i\mathcal{M} \implies & -\frac{\pi^2}{2} \cdot g^4 \cdot \int_0^{1/2} du \cdot u \cdot (1-u) \cdot \int_0^1 d\bar{w} \cdot \\
 & \cdot \int_0^1 \frac{d\bar{v} \cdot \left(1 + \frac{i}{2}\bar{v}\right)}{\left[J_m(\bar{v}=0) - i\varepsilon - i \cdot \left(\frac{1-u}{2}\right)^2 \cdot \bar{v}\right]^2} + \text{IR finite terms.}
 \end{aligned} \tag{33}$$

An elementary decomposition of the integrand helps us to get rid of the square in the denominator

$$i\mathcal{M} \implies \frac{\pi^2}{2} \cdot g^4 \cdot \int_0^{1/2} \frac{u \cdot du}{1-u} \cdot \tag{34}$$

$$\cdot \int_0^1 d\bar{w} \cdot \int_0^1 \frac{d\bar{v}}{J_m(\bar{v}=0) - i\varepsilon - i \cdot \left(\frac{1-u}{2}\right)^2 \bar{v}} \tag{35}$$

+IR finite terms.

We can now do two of the integrals to get

$$i\mathcal{M} \implies -\frac{i\pi^2}{2E^2} \cdot g^4 \cdot \int_0^{1/2} \frac{du}{u \cdot (1-u)} \cdot \frac{[\log(1+i-\sqrt{u}) - \log(1+i+\sqrt{u})] - [\log(i-\sqrt{u}) - \log(i+\sqrt{u})]}{\sqrt{\frac{m^2}{E^2} \cdot \frac{1-u}{u^2} - \beta^2 - i\varepsilon}}. \quad (36)$$

Similar calculations for the region $v : (-i \rightarrow 0)$ and $w : (0 \rightarrow 1-i)$ lead to a similar formula with the numerator replaced by

$$[\log(\sqrt{u} + 1 + i) - \log(\sqrt{u} - 1 - i)],$$

and all other regions end up with no IR divergent contributions. The sum of all IR divergent terms, with the variable $x = \frac{1-u}{u^2}$, is

$$i\mathcal{M} \implies -\frac{i\pi^2}{2E^2} \cdot g^4 \cdot \int_2^\infty \frac{dx}{2x} \cdot \left(1 + \frac{1}{\sqrt{1+4x}}\right) \cdot \frac{\log(i+\sqrt{x}) - \log(i-\sqrt{x}) + i\pi}{\sqrt{\mu^2 x - \beta^2 - i\varepsilon}}. \quad (37)$$

An analysis of the complex x singularities and changing the x contour shows that the $\frac{1}{\sqrt{1+4x}}$ term is IR regular. In the other term we use $y = \frac{\mu^2}{\beta^2} \cdot x$ and with similar tricks we can show that in the resulting formula,

$$i\mathcal{M} \implies -\frac{i\pi^2}{4Ep} \cdot g^4 \cdot \int_{2\frac{m^2}{p^2}}^\infty \frac{dy}{y} \cdot \frac{\log(\frac{i}{\beta} + \sqrt{y-1-i\varepsilon}) - \log(\frac{i}{\beta} - \sqrt{y-1-i\varepsilon}) + i\pi}{\sqrt{y-1-i\varepsilon}} \quad (38)$$

all the IR divergences are contained in a small neighborhood of zero, in an $\int_{\dots}^\eta dy$ region with *any* m -independent $\eta > 0$. Because the fraction in the integrand is an analytic function in $0 \leq y \leq \eta$, the IR divergence is read off easily:

$$i\mathcal{M} \implies \frac{\pi^2}{4Ep} \cdot g^4 \cdot \left[i\pi - \log \frac{1+\beta}{1-\beta} \right] \cdot \log \frac{\eta}{\mu^2}, \quad (39)$$

which, restoring the unit of mass², $-1 \Rightarrow t$, yields Eqn. (21.1).

Acknowledgements

The author is indebted to Prof. J. F. Donoghue for the numerous discussions and helpful comments.

References

- [1] J. M. Cornwall, D. N. Levin, G. Tiktopoulos, Phys. Rev. **D10**, 1145 (1974); C. E. Vayonakis, Lett. Nuov. Cim. **17**, 383 (1976); B. W. Lee, C. Quigg, H. B. Thacker, Phys. Rev. **D16**, 1519 (1977); M. S. Chanowitz, M. K. Gaillard, Nucl. Phys. **B261**, 379 (1985); J. Bagger, C. Schmidt, Phys. Rev. **D41**, 264 (1990).
- [2] C. Grosse-Knetter, Z. Phys. **C67**, 261 (1995).
- [3] H. Veltman, Phys. Rev. **D41**, 2294 (1990).
- [4] H.-J. He et al, hep-ph/9508295, Phys. Rev. **D51**, 6463 (1995), Phys. Lett. **B329**, 278 (1994), Phys. Rev. **D49**, 4842 (1994), Phys. Rev. Lett. **69**, 2619 (1992), Phys. Rev. **D38**, 2237 (2237).
- [5] D. Zwanziger, Phys. Rev. **D11**, 3481 (1975).
- [6] S. Weinberg, Phys. Rev. **B140**, 516 (1965).
- [7] F. Gross, *Relativistic Quantum Mechanics and Field Theory*, Wiley, N.Y., p. 377.
- [8] R. E. Cutkosky, J. Math. Phys. **1**, 429 (1960).